Excited-State Dynamics in the Covalently Linked Systems: Pyrene−$(CH_2)_n$−Aryl Azide†

Nina P. Gritsan,*[,‡,§] Elena A. Pritchina,[‡,§] Igor I. Barabanov,[‡] Gotard T. Burdzinski,[∥,⊥] and Matthew S. Platz[∥]

Institute of Chemical Kinetics and Combustion, Siberian Branch of Russian Academy of Sciences, 3 Institutskaya Street, 630090 Novosibirsk, Russia, Novosibirsk State University, 2 Pirogova Street, 630090 Novosibirsk, Russia, Department of Chemistry, The Ohio State University, 100 West 18th Avenue, Columbus, Ohio 43210, and Quantum Electronics Laboratory, Faculty of Physics, Adam Mickiewicz University, 85 Umultowska, Poznan 61-614, Poland

Received: February 8, 2009; Revised Manuscript Received: March 30, 2009

The primary physical and chemical processes which follow photoexcitation of the covalently linked systems, 1-[(4-azido-2,3,5,6-tetrafluorobenzoyloxy)methyl]pyrene (**2**) and 1-[3-(4-azido-2,3,5,6-tetrafluorobenzoyloxy)-propyl]pyrene (**3**), have been studied using femto- and nanosecond transient absorption spectroscopy and computational chemistry. Excitation of **2** and **3** at 336 nm results in the population of the second excited singlet state of the pyrene moiety (S_2). Internal conversion to the lowest excited singlet state of the pyrene moiety (S_1) occurs with a time constant of ∼140 fs, a value which is similar to that of unsubstituted pyrene. The S_1 local pyrene state, initially formed with excess vibrational energy, undergoes vibrational cooling with a time constant ∼2 ps. The decay of the local pyrene S_1 state measured in the pump−probe experiments was described by a two exponential function with time constants which agree well with the values obtained previously from the fluorescence decay kinetics (Barabanov, I. I.; Pritchina, E. A.; Takaya, T.; Gritsan, N. P. *Mendeleev Commun*. **2008**, *18*, 273). In both systems decay of the local pyrene S_1 state on the time scale of tens of picoseconds is accompanied by formation of a product with a narrow band at ∼460 nm. This transient absorption was assigned to the radical cation of the pyrene moiety. Calculations predict very fast dissociation of the counterpart aryl azide radical anion with formation of the corresponding arylnitrene radical anion. Decay of the local pyrene S_1 state on the longer time scale (hundreds of ps) is not accompanied by formation of a noticeable amount of pyrene radical cation. Most likely, both electron transfer and energy transfer from pyrene to aryl azide moiety are responsible for the photosensitization of the perfluorinated aryl azide decomposition.

1. Introduction

Photoaffinity labeling and cross-linking techniques[1] are widely used to provide structural information for large macromolecular cellular complexes,[2] in situations where high-resolution structural information is not available,[3] and in cases where the dynamics of a system is important.[4] The photoactive group of an affinity reagent is covalently bound to a natural ligand of a biological macromolecule. The photolysis of a complex of a photoaffinity reagent with the target biological macromolecule results in the covalent binding of the ligand and the biomolecule. For example, oligonucleotides are the natural ligands of DNA and RNA.

Aryl azide based[5] photocross-linking and photoaffinity labeling has been widely employed to obtain information on the higher order structure of RNA[6] and RNA−protein complexes[7,8] and DNA−protein[8,9] interactions. Therefore, the aryl azide mediated cross-linking represents a potentially powerful approach for mapping RNA (or DNA) and protein structural neighbors in three-dimensional space,[10] and it seems likely to be an important tool even in the age of proteomics.[11]

Increased specificity for nucleic acid sequences, as well as much higher efficiency, was obtained using "binary" reagents.[12,13] These reagents consist of two tandem oligonucleotides which are complementary to a target sequence of nucleic acid. Each oligonucleotide is covalently linked through its terminal phosphate group with photoreactive or photosensitizing groups.[12] Anthracene, pyrene, and perylene derivatives were used as sensitizers and fluoro-substituted phenylazides were used as photoreagents in binary systems.[12,13] The reaction mixture is irradiated with light, which is not absorbed by aryl azide. Nevertheless, the azido-group undergoes photodecomposition and forms a cross-link with protein either in or at the active site.[12,13] However, the mechanism of sensitization remains unclear, although the knowledge of this mechanism is very important for analysis of the photoaffinity labeling by "binary" reagents.[12,13] If quenching occurs by an energy transfer mechanism, an aryl azide in the singlet excited state is formed, and its subsequent reactions are identical to those taking place upon direct photolysis, the mechanism of the latter being currently well understood.[14] On the other hand, very little is known about redox reactions of aryl azides.[15]

Quenching of pyrene fluorescence by aryl azides, including 4-azido-2,3,5,6-tetrafluorobenzoic acid (**1**), has been studied in solution using fluorescence spectroscopy and nanosecond laser flash photolysis.[16] The formation of pyrene cation has not been detected and the energy transfer mechanism of quenching has been proposed.[16] However, a mechanism involving electron

† Part of the "Hiroshi Masuhara Festschrift".

* To whom correspondence should be addressed. E-mail: gritsan@kinetics.nsc.ru. Tel: 7(383) 333 3053. Fax: 7(383) 330 7350.
‡ Institute of Chemical Kinetics and Combustion.
§ Novosibirsk State University.
∥ The Ohio State University.
⊥ Adam Mickiewicz University.

10.1021/jp901157s CCC: $40.75
Published on Web 04/23/2009

SCHEME 1

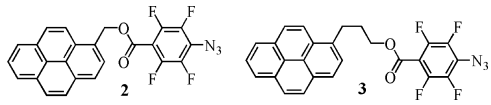

transfer followed by fast N−N bond dissociation and charge recombination could not be excluded. Covalently linking the donor and acceptor residues facilitates the quenching and provides the opportunity to detect primary intermediates, and thus to distinguish between electron and energy transfer mechanisms.

Recently,[17] the synthesis of the covalently linked systems, 1-[(4-azido-2,3,5,6-tetrafluorobenzoyloxy)methyl]pyrene (**2**) and 1-[3-(4-azido-2,3,5,6-tetrafluorobenzoyloxy)propyl]pyrene (**3**), has been performed, and quenching of pyrene fluorescence on a picosecond time scale has been reported. The fluorescence decay kinetics of linked systems **2** and **3** (Scheme 1) were well described by two-exponential ($\tau_1 = 164 \pm 2$ ps and $\tau_2 = 6.9 \pm 0.2$ ns) and three-exponential ($\tau_1 \approx 40$ ps, $\tau_2 = 770 \pm 20$ ps, and $\tau_3 = 3.8 \pm 0.5$ ns) functions, respectively. The contribution of the longest component was found to be small (~0.06) and was proposed to be due to the photoproducts.[17]

To reveal the mechanism of the pyrene fluorescence quenching by aryl azides, a detailed study of photophysics of the covalently linked systems **2** and **3** has been performed using femtosecond transient absorption spectroscopy. In addition, the intermediates produced upon photolysis of aryl azide **1** and binary system **2** were detected using nanosecond laser flash photolysis techniques. The results of our investigations provide new insight into the mechanism of sensitization of aryl azide decomposition in binary reagents.

2. Experimental and Computational Details

Pyrene derivatives **2** (mp 188−190 °C) and **3** (mp 150.5−152.5 °C) were synthesized as described in ref 17 using esterification of azidotetrafluorobenzoic acid **1** by pyren-1-ylmethanol (**4**)[18] and 3-(pyren-1-yl)propan-1-ol,[19] respectively. We chose a special preparative one-stage synthesis of esters from carboxylic acids and alcohols in the presence of Et_3N, promoted by 1-methyl-2-chloropyridinium iodide (Mukaiyama reagent).[20] The advantage of this method is the absence of acidic catalysts and the ambient temperature of synthesis, which is important for very reactive and labile azido-derivatives.[21]

Electronic absorption spectra were recorded on a UV−vis Shimadzu 2401 spectrometer. Prior to the spectroscopic experiments, pyrene derivatives **2** and **3** were additionally recrystallized from $CHCl_3$. Pyren-1-ylmethanol (**4**)[18] was purified by chromatography (silica gel, eluent: benzene) and treated with activated carbon, and finally recrystallized from a benzene-hexane mixture. 4-Azido-2,3,5,6-tetrafluorobenzoic acid (**1**) from Aldrich was used without additional purification.

Luminescence spectra were recorded in the analog mode using an 8-bit digital oscilloscope (ISA BUS CompuScope) from Gage Applied Sciences, which was directly interfaced to a personal computer. A 313 nm line of a high-pressure mercury lamp was isolated using a high-aperture monochromator and a combination of glass filters and used for fluorescence excitation. The experimental luminescence spectra were corrected taking into account the spectral sensitivity of the system, which was measured using quinine bisulfate as a luminescent standard.[22]

Femtosecond Broadband UV−Vis Transient Absorption Experiments. Ultrafast experiments were performed in acetonitrile at room temperature. The absorbance of the sample solutions was about 0.5 (in 1 mm cell) at an excitation wavelength (336 nm). Transient absorption spectra were recorded on a femtosecond broadband UV−vis transient absorption spectrometer.[23] The laser system consists of a short pulse titanium-sapphire oscillator (Coherent, Mira) followed by high-energy titanium-sapphire regenerative amplifier (Coherent, Positive Light, Legend HE USP). The main part of the beam is used to pump an OPA (OPerA Coherent). A small part of the fundamental beam is focused into a 1 mm thick calcium fluoride plate to generate a white light continuum between 340−640 nm. The white light continuum is split into probe and reference beams of nearly equal intensity. The probe and reference beams pass through the sample, but only the probe overlaps with the pump beam in the sample. The pump pulse energy was about 6 μJ at the sample position. The sample is circulated in a Harrick Scientific flow cell (1 mm thick CaF_2 windows, optical path length 1 mm).

The detection system consists of an imaging polychromator (Triax 550 Jobin Yvon) and CCD camera (Symphony Jobin Yvon). Transient absorption spectra were registered at different pump−probe delay times using an optical delay line. To gauge the reproducibility of the data the entire set of pump−probe delay positions was repeated at least three times. To avoid rotational-diffusion effects, the angle between polarizations of the pump beam and the probe beam was set to the magic angle (54.7°).[24] Transient absorption spectra were corrected for chirp in the probe continuum.[25]

Kinetic traces were analyzed by fitting to a sum of exponential terms. Convolution with a Gaussian response function was included in the fitting procedure. The instrument response (fwhm) time was approximately 190 fs.

Nanosecond Laser Flash Photolysis (LFP). A Nd:YAG laser (Spectra Physics LAB-150-10, 266 and 355 nm, 5 ns, 30 mJ) was used as the excitation light source. The spectrometer has been described previously.[26] Solutions of **1** and **2**, **3** were prepared in spectroscopic grade acetonitrile with an optical density (OD) of about 1.0 at 266 nm and 0.3 at 355 nm, respectively. Experiments were performed at ambient temperature (~295 K).

Quantum Chemical Calculations. The geometries of pyrene, azide **1**, their cations and anions, and linked systems **2** and **3** were optimized by the B3LYP method[27] with the 6-31G(d) or 6-31+G(d) basis sets. All equilibrium structures were ascertained to be minima on potential energy surfaces. The electronic absorption spectra (EAS) were calculated by the time-dependent TD-B3LYP/6-31+G(d) technique.[28] All calculations were performed with the Gaussian 03[29] suite of programs. The influence of the solvent was taken into consideration using the PCM[30] model as implemented to Gaussian 03.

Excited state energies for pyrene were also calculated at the B3LYP/6-31G(d) geometry by the CASSCF/CASPT2 procedure[31] with the ANO-S basis set of Pierloot et al.[32] using the MOLCAS program.[33] In order to arrive at a satisfactory description of all excited states at the CASPT2 level (i.e., remove intruder states), it was necessary to resort to the level-shifting technique,[34] whereby it was carefully ascertained that no artifacts are introduced. The active spaces used in these calculations are described in the Supporting Information and depicted in Figure S1.

The enthalpy and free energy changes for decomposition of the azide **1** anion to the anion of corresponding nitrene and molecular nitrogen, and the driving force of the direct and reverse electron transfer were estimated at the B3LYP/6-31+G(d) level of theory.

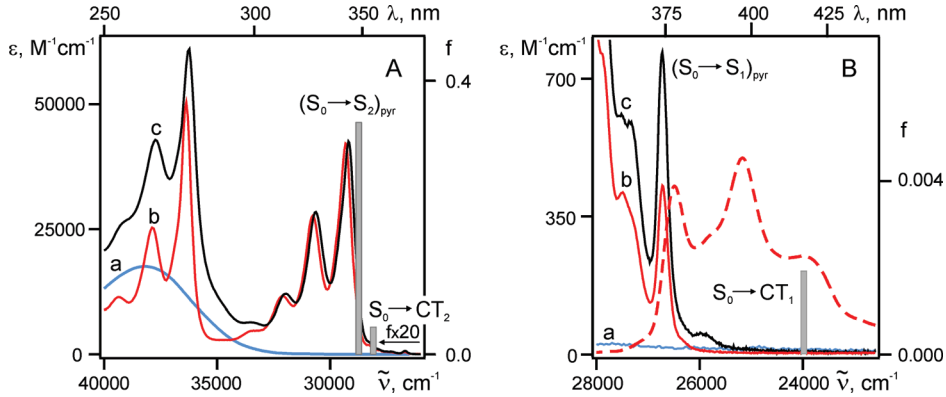

Figure 1. UV−vis spectra of aryl azide **1** (a, blue), pyren-1-ylmethanol **4** (b, red), and covalently linked system **2** (c, black) in CH_3CN at room temperature in the ranges 250−370 (A) and 355−440 nm (B). Red dashed line describes fluorescence spectrum of **4** in CH_3CN at room temperature. The long wavelength transitions in the electronic absorption spectrum of **2** calculated at the B3LYP/6-31+G(d) level are depicted as gray bars. The traces a−c have been adapted from ref 17.

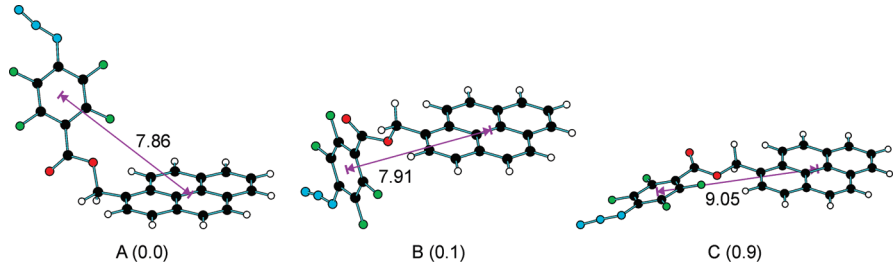

Figure 2. Structures of the lowest energy conformations (**A**−**C**) of the covalently linked system **2** optimized at the B3LYP/6-31G(d) level of theory (atoms are depicted as follows: C, black; N, blue; O, red; F, green; and H, white). The distances between centers of pyrene and aryl moieties are depicted in Å. The relative Gibbs free energies of the conformations in acetonitrile at 298 K are given in parentheses (in kcal/mol). Structures A and B have been adapted from ref 17.

3. Results and Discussion

3.1. Electronic Absorption Spectra and Structures of the Covalently Linked Systems 2 and 3. Figure 1 displays the electronic absorption spectra of azide **1**, pyrenylmethanol **4**, and covalently linked system **2**. Figure 1A demonstrates that the spectrum of pyrene derivative **2** is very close to the sum of the spectra of azide **1** and pyrenylmethanol **4**, although the maxima of the vibrational progression of **2** are slightly (1.5 nm) shifted to the red. The difference in the spectra of substituted pyrenes **2** and **4** is more pronounced at the red edge where aryl azide **1** has no noticeable absorption (Figure 1B).

Figure 1B displays also the fluorescence spectrum of **4**. From the crossing point of the absorption and fluorescence spectra, the energy of the 0−0 transition to the S_1 state of **4** could be calculated as 3.302 ± 0.005 eV (Figure 1B). The fluorescence lifetime of **4** was measured to be 200 ± 10 ns. We have failed to detect the fluorescence spectrum of **2**. This coincides well with very efficient quenching of fluorescence in the linked system **2** (τ = 164 ± 2 ps).[17]

It is clear from Figure 1B that the transition to the first excited singlet state of **4** (S_1, 0−0 band at 374 nm) has very low oscillator strength and is masked by the tail of more intense transition to the second excited state (S_2, λ_{max} = 341 nm). The UV−vis spectrum of **4** is almost identical to the spectrum of pyrene (Supporting Information, Figure S2). High quality CASSCF(14,14)/CASPT2 calculations of the pyrene UV−vis spectrum have been performed (Supporting Information, Figure S1) and vertical transitions to the S_1 (1^1B_{2u}) and S_2 (1^1B_{1u}) states were predicted and appeared to be in fairly good agreement with experiment (Figure S2). Pyrene and its substituted analogues (**2**−**4**) could be directly excited to the S_1 state using light with $\lambda \geq$ 370 nm. However, absorption of pyrene and its derivatives in this region is too low and excitation to the S_2 state is commonly accepted for the study of spectroscopy and photophysics of substituted pyrenes.[17,35−38] In our ultrafast experiments we also employed excitation to the S_2 state (λ_{ex} = 336 nm).

A set of minima, corresponding to different conformations, were localized at the potential energy surface (PES) of **2**. Figure 2 presents the structures, corresponding to the conformers with the lowest Gibbs free energies. All other conformations have significantly higher formation enthalpies and Gibbs free energies than **2A** ($\Delta(\Delta G) \geq$ 7.5 kcal/mol). Thus, calculations predict that compound **2** exists mainly in two conformations: **2A** and **2B**. Transition states for the interconversion between conformers **2A**−**2C** were also localized. The free energies of activation for the interconversion of conformers were found to be 6.8 kcal/mol (**2A** → **2B**), 2.4 kcal/mol (**2B** → **2C**), and 2.8 kcal/mol (**2A** → **2C**). According to the calculations, the characteristic time of interconversion between conformers **2A** and **2B** in the ground state is about 5 ns. Similar time constant ought to be expected in the excited state with excitation localized on the pyrene chromophore.

The electronic absorption spectra of the conformers **2A**−**2C** have been calculated by the time-dependent B3LYP/6-31+G(d) technique. Calculations predict that comparing to **4,** the covalently linked system **2** has two additional low intensity transitions in the near-UV region. These transitions involve electron excitations from the HOMO, localized on the pyrene fragment, to the LUMO or LUMO+2 localized on the aryl azide fragment (Figure 3). Thus, these electronic transitions correspond to the excitation to the charge-transfer states (CT_1 and CT_2). It is well-known[28] that TD-DFT significantly underesti-

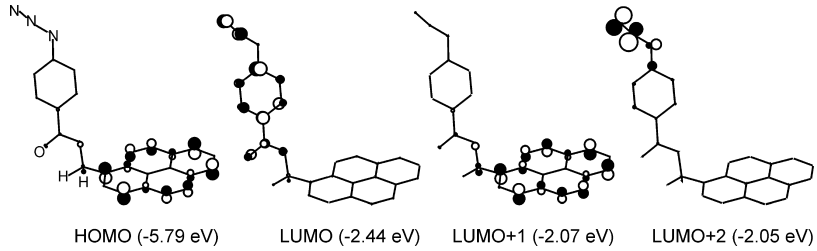

Figure 3. HOMO and first three vacant MOs of 1-[(4-azido-2,3,5,6-tetrafluorobenzoyloxy)methyl]pyrene (**2**) and their energies calculated at the B3LYP/6-31+G(d) level. The frontier MOs have been adapted from ref 17.

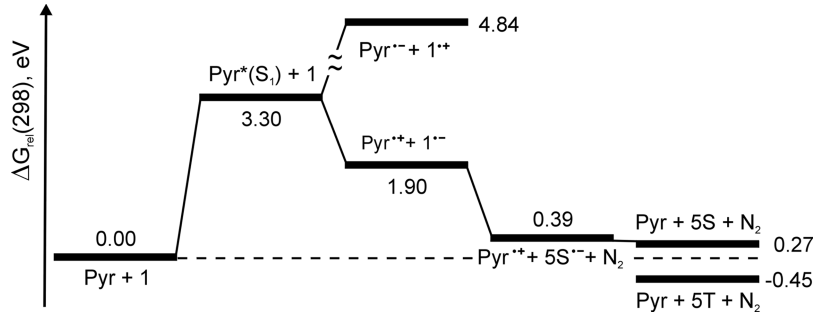

Figure 4. Free energy diagram (ΔG_{rel}, eV) for the electron transfer and subsequent reactions in the pair of pyrene (Pyr) and 4-azido-2,3,5,6-tetrafluorobenzoic acid (**1**) in acetonitrile (**5S** and **5T** are the singlet and triplet 4-nitreno-2,3,5,6-tetrafluorobenzoic acid, Scheme 2). The distance between centers of the ions was chosen to be 8 Å as in the linked system **2**.

mates excitation energies of CT states, although application of hybrid functionals slightly improves results of calculations.

Figure 1 displays positions and oscillator strengths of the electronic transitions calculated for the thermodynamically favorable conformer **2A**. Indeed, calculations underestimate energy of the CT_1 state. However, the difference in the spectra of **2** and **4** (Figure 1B) can be explained by the transition to CT_1 state in former compound. Note that the oscillator strength of this transition depends on conformation (Supporting Information, Table S2).

A bigger set of minima, corresponding to different conformations, were localized at the PES of **3**. The structures, corresponding to four conformers with the lowest free energies (**3A**−**3D**), are presented in the Supporting Information (Figure S3). According to the calculations, the lowest energy conformation (**3A**) has a rather long distance between the centers of pyrene and aryl azide moieties (10.4 Å). Conformers **3B**−**3D** are characterized by a higher free energy (by 0.2−0.7 kcal/mol), but have essentially the same distances between moieties (10.3−10.6 Å). All other conformers have much higher free energy than that of **3A** ($\Delta(\Delta G) > 1$ kcal/mol) and distances between moieties in the range 4.2−11.6 Å. The structures of folded conformations of **3** are also presented in the Supporting Information (**3E**−**3G**, Figure S4).

As in the case of **2**, time-dependent DFT calculations predict two transitions to CT states in the near-UV spectrum of **3** (Supporting Information, Table S2). Table S2 (Supporting Information) demonstrates that oscillator strengths of transitions to CT_1 states are about an order of magnitude lower than those for **2**. Thus, the oscillator strengths of transitions to CT_1 states depend on both the distance between moieties and their mutual orientation.

3.2. Estimation of the Driving Force of the Electron Transfer Process in Linked Systems. Electron transfer (ET) is one of the most important and well investigated chemical reactions.[39] Moreover, a theory of electron transfer has been elaborated in the classical and quantum mechanical formulations.[39,40] Thus, ET rate constants and their dependences on donor and acceptor properties and solvent polarization could be analyzed and even predicted in some cases. In the framework of the classical Marcus approach,[39] the ET rate constant (k_{ET}) is given by the expression

$$k_{ET} = A \exp\left[\frac{-(\Delta G^0 + \lambda)^2}{4\lambda k_B T}\right] \quad (1)$$

where k_B is the Boltzmann constant, ΔG^0 is the free energy of the ET reaction, and λ is the reorganization energy.

The driving force of the electron transfer reaction ($-\Delta G^0$) could be estimated by the Rehm−Weller formula[39c] using the oxidation potential of the donor and the reduction potential of the acceptor. Unfortunately, the information on redox potentials of aryl azides is extremely scarce.[41] A one-electron reduction potential was reported for *p*-nitrophenyl azide.[15b] A two electron reduction wave and a one-electron reoxidation wave were detected for acetonitrile solution of 4-[(dimethylamino)carbonyl]phenyl azide.[42] To the best of our knowledge, there are no data on redox potentials of the polyfluorinated aryl azides, including azide **1**.

Previously,[16] we estimated the driving force for the proposed photoinduced electron transfer reactions in the pair of pyrene and tolyl azide using quantum chemical calculations. Free energies of pyrene, tolyl azide, and corresponding cations and anions have been calculated using the density functional theory at the hybrid B3LYP level. The PCM model has been used to account for the free energy of solvation. Similar approach was employed to estimate the driving force of the photoinduced ET in the pair pyrene−azide **1** (Figure 4). Figure 4 demonstrates that electron transfer from azide **1** to pyrene in the S_1 state is thermodynamically very unfavorable, $\Delta G^0 = 1.54$ eV. In turn, calculations predict significant driving force ($-\Delta G^0 = 1.4$ eV) for the photoinduced ET from pyrene to azide **1**.

Reorganization energy λ in the formula (1) is a sum of two components: the intramolecular reorganization energy (λ_{in}) and the solvent reorganization energy (λ_s). The latter term can be estimated using a simple formula proposed by Marcus.[39a,b]

SCHEME 2

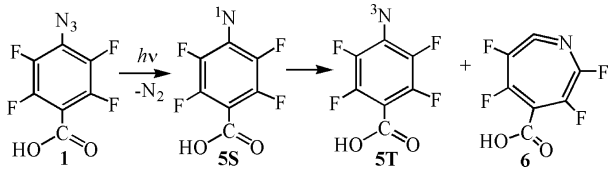

Effective radii of pyrene cation (4.8 Å) and azide anion (4.6 Å) were obtained using quantum chemical calculations and value of λ_s was estimated to be 0.67 eV. Value of λ_{in} has been estimated as described in ref 43

$$\lambda_{in}(T) = \lambda_{in}^{\infty}\left[\frac{4k_BT}{h\nu_{in}}\tanh\frac{h\nu_{in}}{4k_BT}\right] \quad (2)$$

where λ_{in}^{∞} is a high-temperature limit of intramolecular reorganization energy, ν_{in} is an effective oscillation frequency of the degrees of freedom involved in reorganization, and T is temperature.

The value of λ_{in}^{∞} for the pair pyrene−azide **1** has been calculated by the B3LYP/6-31+G* method and found to be 1.05 eV. The contribution of azide **1** to this reorganization energy is dominating with N−N bond length and N−N−N bond angle being changed significantly (0.16 Å and 45°, respectively) on reduction of **1** (Supporting Information, Figure S5). Moreover, the normal modes with ν = 683, 747, and 839 cm^{-1} are mainly involved in this reorganization. Thus, the average frequency ∼750 cm^{-1} was chosen as ν_{in}. At room temperature λ_{in} was estimated to be 0.84 eV and total reorganization energy λ to be 1.51 eV. According to our estimations activation energies of the proposed ET reactions in the linked systems **2** and **3** are close to zero (E_a ∼ 0.05 kcal/mol). Therefore, quenching of the local pyrene fluorescence in these systems through the ET mechanism can proceed on a picosecond time scale.

On the other hand, the energy transfer mechanism can also be operative.[16,17] Indeed, according to the calculations the first excited singlet state (S_1) of phenyl azide and its simple derivatives is dissociative toward the formation of molecular nitrogen and singlet nitrene.[44] Usually, the $S_0 \rightarrow S_1$ transitions in UV spectra of aryl azides manifest themselves as weak long asymmetric tails,[16,42] which is typical of the excitation to dissociative states. The $S_0 \rightarrow S_1$ transition of azide **1** at 309 nm is also dissociative and is characterized as $\pi \rightarrow$ (in plane, π^*) excitation.[17]

Due to the dissociative nature of the S_1 state of azide **1**, its energy cannot be precisely defined. Thus, energy transfer to the local dissociative state of the aryl azide moiety cannot be excluded. Note, that the Foerster mechanism of energy transfer was previously excluded[16] on the basis of the negligible overlap between the pyrene fluorescence and aryl azide absorption spectra. Unfortunately, it is impossible to estimate theoretically the rate constant of energy transfer in the pair pyrene−azide **1** by the Dexter (exchange) mechanism.[45]

To investigate primary processes that follow photoexcitation of pyrene moiety and to shed light on the mechanism of quenching, we investigated photophysics of the covalently linked systems **2** and **3** using femtosecond transient absorption spectroscopy.

3.3. Femtosecond Transient Absorption Spectroscopy of Covalently Linked Systems 2 and 3. A solution of **2** in acetonitrile was pumped by a femtosecond laser pulse (336 nm). As mentioned above, excitation at 336 nm results in the population of the second local excited state of pyrene moiety. The transient absorption spectra produced by excitation of solutions of **2** were recorded at different time delays between the probe and pump pulses. The transient absorption spectra, recorded over a −0.3 to +1 ps time window, are presented in Figure 5A. Figure 5A demonstrates that around time-zero a transient absorption band with maximum at ∼590 nm rises within the laser pulse. After a delay of several hundred femtoseconds, a second band is seen rising with a maximum at ∼475 nm. Note that spectral changes of Figure 5A are very similar to those recorded previously in the pump−probe experiments with pyrene.[38] Thus, as in the case of pyrene, excitation of **2** at 336 nm populates the S_2 local excited state of pyrene moiety, which has an absorption maximum at 588 nm (580 nm in pyrene[37,38]). This state undergoes ultrafast internal conversion into the S_1 local excited state with an absorption maximum at 476 nm (470 nm in pyrene[36−38]).

The transient absorption spectra, recorded over a 1−600 ps time window, are presented in Figure 5B. Figure 5B demonstrates that the transient absorption decays on a picosecond time scale. The final spectrum detected at 600 ps remains practically unchanged until 2.5 ns (maximum time interval available with our setup). Its origin will be discussed below. A small contribution from the stimulated emission around 400 nm cannot be excluded.

Kinetic traces recorded in the available spectral range (400−640 nm) were analyzed using three exponential functions and a convolution using a Gaussian response function. The global fitting yields the following time constants: 150 ± 50 fs, 2.6 ± 0.5 ps, and 110 ± 30 ps. Figure S6 (Supporting

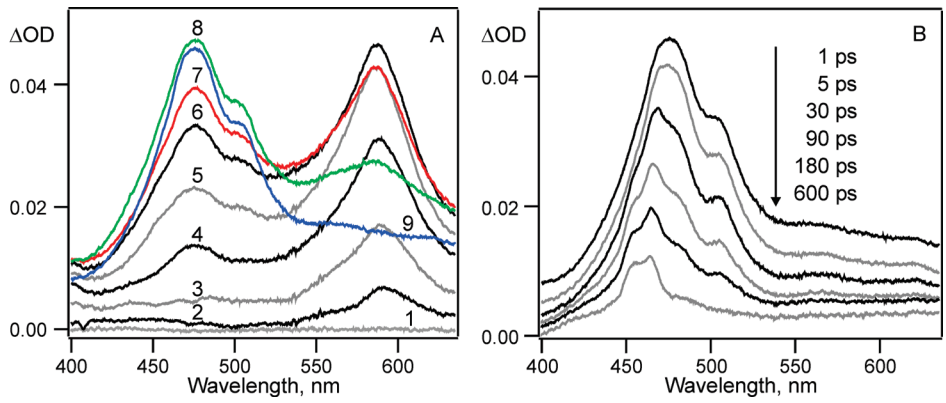

Figure 5. Transient absorption spectra of 1-[(4-azido-2,3,5,6-tetrafluorobenzoyloxy)methyl]pyrene **2** in acetonitrile at ambient temperature recorded at different time delays (ps): (A) −0.3 (1), −0.1 (2), −0.05 (3), 0.0 (4), 0.05 (5), 0.1 (6), 0.15 (7), 0.30 (8), and 1.0 ps (9) and (B) over a 1−600 ps time window.

Information) demonstrates that three exponential fitting reproduces fairly well available experimental kinetics. The shortest time constant (150 ± 50 fs) is assigned to the primary process, $S_2 \rightarrow S_1$ internal conversion (IC). This time constant is close to the value measured previously for unsubstituted pyrene (150 ± 50 fs and ~75 fs).[37,38]

The process with the lifetime of 2.6 ps is characterized by a significant decay of absorption at the long wavelength region (≥500 nm) along with a narrowing of the band (the normalized spectra are presented in the Supporting Information, Figure S7). This pattern is characteristic of a vibrational cooling (VC) of species initially formed with excess vibrational energy.[46] The 2.6 ps time constant is consistent with other reports of VC of polyatomic molecules.[47] Note that the time constant of vibrational cooling in the S_1 state of pyrene was measured to be ~4 ps in *n*-octane.[36]

The time constant 110 ± 30 ps can be assigned to the decay of the local pyrene S_1 state. Indeed, this value is in satisfactory agreement with the time of the fluorescence decay (τ = 164 ± 2 ps),[17] although it is noticeably shorter than the latter value.

However, careful analysis of the transient absorption kinetics on the picosecond time scale (10−600 ps, Supporting Information, Figure S8) demonstrates that kinetic traces can be better fitted by a biexponential function. Thus, we analyzed available kinetic traces using four exponential time dependence and a convolution with a Gaussian response function (Figure 6A−C). The global fitting yields the following time constants: 140 ± 50 fs and 1.7 ± 0.5, 26 ± 5, and 140 ± 20 ps. Thus, adding a fourth exponent does not significantly influence the obtained values of the time constants for the IC and VC processes. Note, that the latter time constant (140 ± 20 ps) is in good agreement with the time of the fluorescence decay (τ = 164 ± 2 ps).[17]

Decay associated spectra (DAS) corresponding to the four exponential time dependence of the experimental kinetic traces are presented in Figure 7. The component a_1 associated with a 140 fs time constant corresponds to the decay of the S_2 absorption band (λ_{max} = 588 nm) and concomitant formation of the S_1 absorption band (λ_{max} = 476 nm) of pyrene moiety (Figure 7A). Very interesting and unexpected conclusion could be done on the basis of the DAS displayed in Figure 7B. Comparing the components a_3, a_4, with a_5, one can conclude that the final spectrum a_5 is formed mainly with a shorter time constant (~26 ps). Moreover, the sum of the a_3 and a_5 components has spectrum similar to that of component a_4. The origin of these peculiarities will be discussed below.

Similar transient absorption spectra were detected in the pump−probe experiments with a solution of **3** (Figure 8). Thus, as in the case of **2** and unsubstituted pyrene, excitation of **3** at 336 nm populates the S_2 local excited state of pyrene moiety, which has an absorption band maximum at ~590 nm (Figure 8A). This state undergoes ultrafast internal conversion into the S_1 local excited state with an absorption band maximum at ~480 nm. Changes in the transient absorption spectrum of **3** over a picosecond time scale are displayed in Figure 8B. The spectra of this figure are similar to those of Figure 5B except for the more resolved structure in the 450−530 region. Note that the spectrum detected 2.5 ns after excitation of **3** (Figure 8B) is similar to the spectrum recorded 600 ps after excitation of **2** (Figure 5B). The origin of these spectra will be discussed below.

As in the case of **2**, the decay kinetics on a picosecond time scale can be described by three-exponential functions. Thus, we analyzed available kinetic traces using four exponential time dependence and a convolution with a Gaussian response function

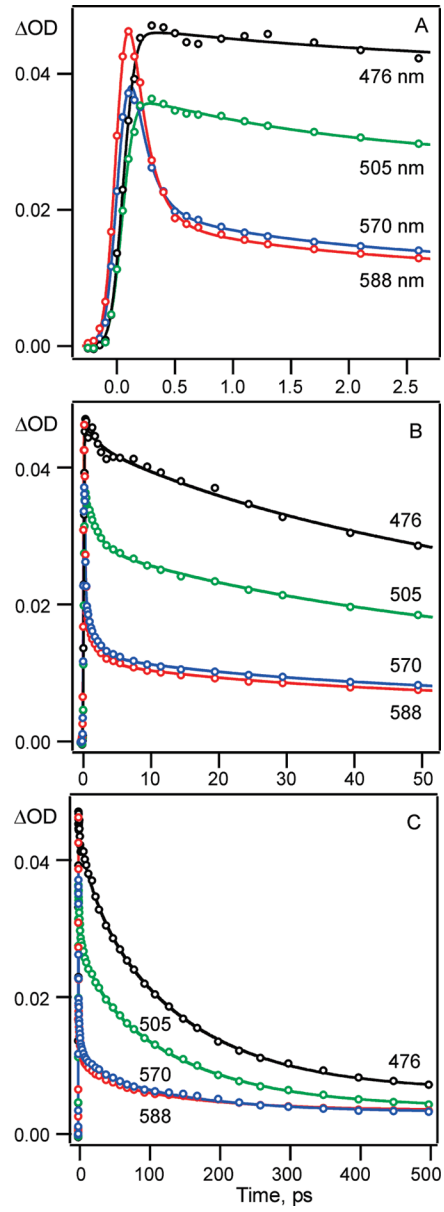

Figure 6. Transient absorption kinetic traces (open circles) for **2** in acetonitrile at 476, 505, 570, and 588 nm fitted to a 4-exponential function (solid lines). Global fitting yields 0.14, 1.7, 26, and 143 ps time constants. Graphs show data in the time windows −0.3 to +3 ps (A), −1 to +50 ps (B), and −5 to +500 ps (C).

(Supporting Information, Figure S9). The global fitting yields the following time constants: 140 ± 50 fs and 1.8 ± 0.5, 46 ± 15, and 810 ± 90 ps. The time constant of the $S_2 \rightarrow S_1$ internal conversion is close to the value measured for **2** and to the well-known value for unsubstituted pyrene (150 ± 50 fs and ~75 fs).[37,38] Vibrational cooling of the local pyrene S_1 state of **3** proceeds with the same time constant as in **2**. The time constants of a two-exponential decay of the pyrene-localized S_1 state (46 ± 15 ps and 810 ± 90 ps) are in very good agreement with a two-exponential fluorescence decay of **3** with the time constants of ~40 and 770 ± 50 ps.[17] Similar to the case of **2**, the decay associated spectra (DAS) indicate (Supporting Information, Figure S10) that the final spectrum a_5 is formed mainly with a shorter time constant (~46 ps). This feature will also be discussed below.

Prior to assignment of the final spectra of Figures 5B and 8B, we will consider the results of the nanosecond laser flash photolysis of aryl azide **1** and covalently linked system **2**.

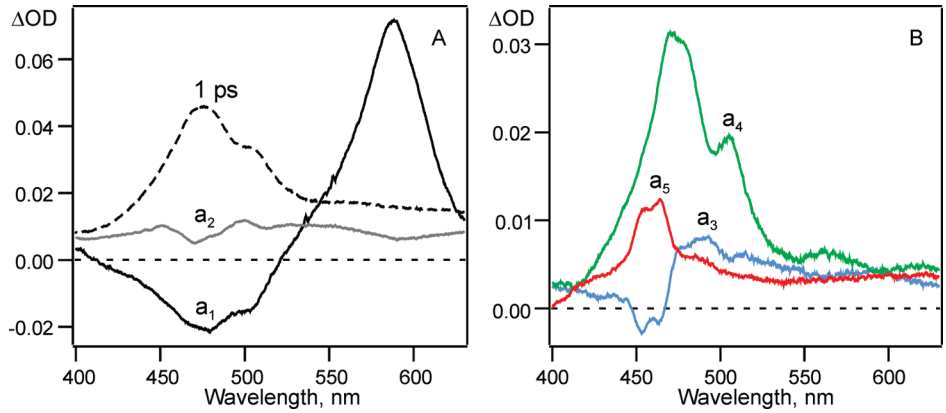

Figure 7. Decay associated spectra (DAS) obtained for 1-[(4-azido-2,3,5,6-tetrafluorobenzoyloxy)methyl]pyrene **2** in acetonitrile at ambient temperature (a_1, component associated with the time constant 140 fs; a_2, 1.7 ps; a_3, 26 ps; a_4, 140 ps; a_5, spectrum at 600 ps). The transient absorption spectrum recorded at 1 ps time delay is displayed for comparison (A).

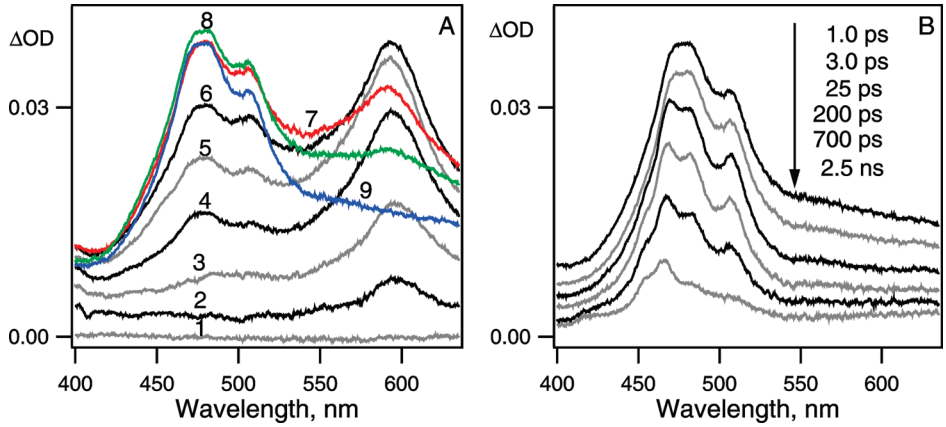

Figure 8. Transient absorption spectra of 1-[3-(4-azido-2,3,5,6-tetrafluorobenzoyloxy)propyl]pyrene (**3**) in acetonitrile at ambient temperature recorded (A) at different time delays (ps): −0.3 (1), −0.1 (2), −0.05 (3), 0.0 (4), 0.05 (5), 0.1 (6), 0.2 (7), 0.30 (8), and 1.0 (9), and (B) over a 1−2500 ps time window.

3.4. Laser Flash Photolysis Study of Arylazide 1 and Covalently Linked System 2. The details of the photochemistry of aryl azides are now well understood, primarily, as a result of the application of the nanosecond laser flash photolysis techniques and high level quantum chemical calculations.[14] The influence of substituents on the electronic absorption spectra and reactivity of substituted phenylnitrenes, the primary products of the aryl azide photolysis, has been analyzed in details.[14] It was demonstrated[48,49] that the *ortho,ortho*-difluoro substitution prolongs the lifetime of the singlet arylnitrene significantly (by more than 2 orders of magnitude). The long lifetime of the polyfluorinated singlet arylnitrenes explains their rich bimolecular chemistry.[14,49] Therefore, polyfluorinated aryl azides are indeed more useful in aryl azide based photocross-linking and photoaffinity labeling than their nonfluorinated counterparts.

To record the spectra of the singlet and triplet 4-nitreno-2,3,5,6-tetrafluorobenzoic acid (**5S**, **5T**), a solution of azide **1** in acetonitrile was pumped by a nanosecond laser pulse (266 nm). Figure 9A (spectrum 1) displays the transient absorption spectrum recorded 800 ns after laser pulse. This spectrum is similar to the transient absorption spectra recorded previously for some polyfluorinated aryl azides, which were assigned to a mixture of the spectra of corresponding triplet arylnitrene ($\lambda_{max} \sim 400$ and 550 nm) and azepine ($\lambda_{max} \sim 400$ nm).[14a,48,49] The persistent spectrum of the triplet nitrene **5T** detected after brief photolysis of **1** at 77 K is presented in the Supporting Information (Figure S11, $\lambda_{max} = 313$, 401, 420, and 573 nm). Thus, the spectrum 1 of Figure 9A could also be assigned to the mixture of triplet nitrene **5T** and azepine **6** (Scheme 2).

Spectrum 2 of Figure 9A belongs to the precursor of the triplet nitrene **5T** and azepine **6** and can be unambiguously assigned to the singlet nitrene **5S**. Indeed, this spectrum is similar to the spectra of other polyfluorinated singlet arylnitrenes[49b−d] and has a lifetime at ambient temperature (200 ± 20 ns) typical of such nitrenes.[48,49]

The transient absorption spectrum recorded 50 μs after the laser excitation of **1** (Figure 9B, spectrum 1) is typical of formation of azobenzenes,[48,50] which are the products of triplet arylnitrene recombination.[14] A similar spectrum, but with two maxima (Figure 9B, red curve), was detected 50 μs after the laser excitation of **2**. The shape of the latter spectrum could be explained by a superposition of the transient absorption characteristic of azo-compound formation (former spectrum) and depletion of the absorption of **2** (Figure 9B, spectrum 3), which is due to the pyrene moiety. Unfortunately, the nanosecond laser flash spectrometer[26] has relatively poor spectral resolution, and the depletion of the spectrum with pronounced structure reveals a structureless hole in the spectrum. The difference spectrum recorded upon a stationary photolysis of **2** is presented in the Supporting Information (Figure S12).

In accord with azo-compound formation, the spectrum detected 700 ns after the laser excitation of **2** (Figure 9A, spectrum 3) is characteristic of polyfluorinated triplet arylnitrenes.[49] Note, that the depletion of the starting material is also pronounced in this spectrum. LFP experiments performed on

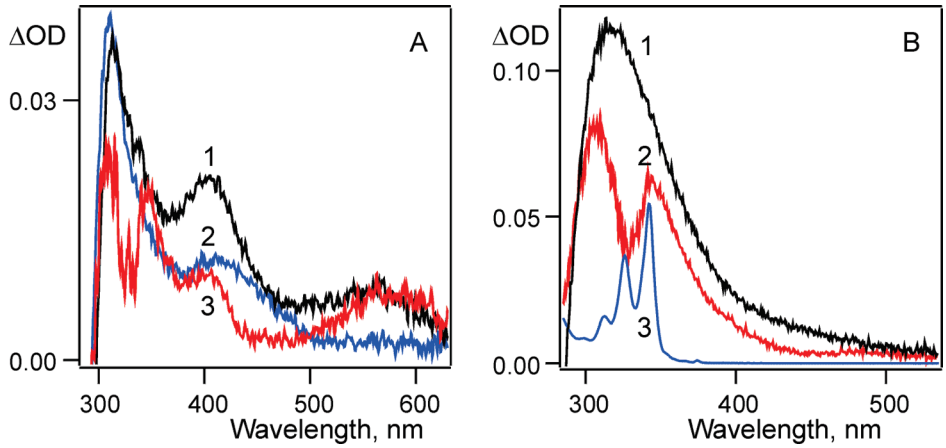

Figure 9. (A) Transient absorption spectra recorded 800 (1) and 70 ns (2) after laser excitation (λ_{ex} = 266 nm) of 4-azido-2,3,5,6-tetrafluorobenzoic acid **1** and 700 ns (3) after laser excitation (λ_{ex} = 355 nm) of the covalently linked system **2** in acetonitrile at ambient temperature. (B) Transient absorption spectra recorded 50 μs after excitation of **1** (spectrum 1, λ_{ex} = 266 nm) and **2** (spectrum 2, λ_{ex} = 355 nm). Spectrum 3 is a stationary UV−vis spectrum of compound **2**.

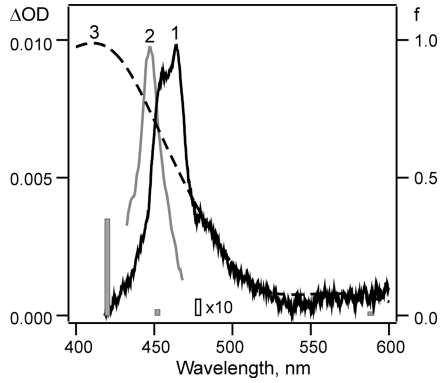

Figure 10. Transient absorption spectra recorded in acetonitrile at ambient temperature (1) 600 ps after the fs excitation of 1-[(4-azido-2,3,5,6-tetrafluorobenzoyloxy)methyl]pyrene **2**, (2) 50 ns after laser excitation (λ_{ex} = 355 nm) of pyrene,[16] and (3) 70 ns after laser excitation (λ_{ex} = 266 nm) of 4-azido-2,3,5,6-tetrafluorobenzoic acid **1**. The electronic transitions in the UV−vis spectrum of the pyrene radical cation and arylnitrene radical anion (^{2}**5S**$^-$) calculated at the UB3LYP/6-31+G(d) level in acetonitrile are depicted as gray and open bars, respectively.

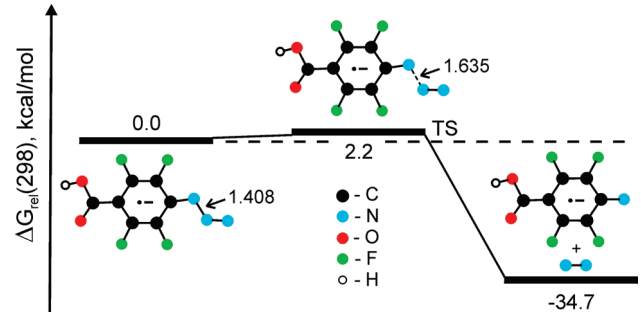

Figure 11. Relative Gibbs free energies of the stationary points on the PES for dissociation of the azide **1** radical anion (^{2}**1**$^-$) (atoms are depicted as follows: C, black; N, blue; O, red; F, green; and H, white). The N−N bond lengths are given in Å.

the linked systems **2** and **3**, as well as product analysis, are now in progress and results will be published elsewhere.

4. Discussion

As the electronic absorption spectra of the singlet arylnitrene **5S** and the radical cation of pyrene[16,52] are known, we can compare them with the transient absorption spectra detected after completion of quenching of the pyrene S_1 local state (Figures 5B and 8B).

Figure 10 demonstrates that the spectrum of singlet nitrene **5S** (3) is much broader and shifted significantly to the blue compared to the spectrum 1. On the contrary, the spectrum of pyrene cation (2) has a similar shape and is shifted to the blue only slightly (~15 nm). Thus, the transient absorption spectra formed upon quenching of the pyrene local S_1 state of **2** and **3** (Figures 5B and 8B) can be assigned mainly to the radical cation of the pyrene moiety. The experimental band is slightly broadened compared to the band of the free radical cation of pyrene (Figure 10) because of the interaction with radical anion in the linked system.

Along with the radical cation of the pyrene moiety, the radical anion of the aryl azide moiety should be formed. It is known from the literature[15] that reduction of aryl azides yields arylnitrene radical anions. However, there is no information on the rate constants of dissociation of aryl azide radical anions as well as the electronic absorption spectra of radical anions of aryl azides and nitrenes. Thus, we estimated the rate constant of the dissociation of the radical anion ^{2}**1**$^-$ using theory.

Using the UB3LYP/6-31+G(d) method, we localized the transition state (Figure 11) for dissociation of ^{2}**1**$^-$ and found that the Gibbs free energy of activation ($\Delta G^{\#}$) of this reaction is very low in both the gas phase (1.0 kcal/mol) and acetonitrile (2.2 kcal/mol). Using the latter value and formula (3), the rate constant of dissociation (k_{diss}) was predicted to be 1.6×10^{11} s^{-1}. Thus, calculations predict that the aryl azide radical anion undergoes very fast dissociation to yield an arylnitrene radical anion.

$$k_{diss} = k_B T/h \exp(-\Delta G^{\#}/RT) \quad (3)$$

Arylnitrene radical anions have never been detected using electronic absorption spectroscopy. Our calculations using the time dependent UB3LYP/6-31+G(d) technique predict that radical anion ^{2}**5S**$^-$ has absorption band in the visible region (Figure 10, open bar) with a maximum at 478 nm. However, the oscillator strength of this transition is about 50 times lower than that calculated for the corresponding transition of the pyrene radical cation (Figure 10, gray bar). Nevertheless, the contribution of the absorption of ^{2}**5S**$^-$ to the experimental spectrum (Figure 10, spectrum 1) cannot be excluded.

Most likely, formation of the covalently linked pyrene radical cation and arylnitrene radical anion will be followed by back

electron transfer (BET). Our DFT calculations predict that the BET in the pair of pyrene radical cation and ^{2}**5S**$^-$ radical anion (^{2}Pyr$^+$ + ^{2}**5S**$^-$ → Pyr + **5S**) in acetonitrile is an exothermal reaction ($\Delta G^0 = -0.12$ eV, Figure 4).

As estimated in the section 3.2, the driving force of photoinduced electron transfer from pyrene to azide **1** is very high ($-\Delta G^0 = 1.4$ eV) and this process is predicted to be barrierless. Hence, it may proceed on a picosecond time scale and the decay of the local pyrene S_1 state can result in formation of covalently linked pyrene radical cation and aryl azide radical anion.

However, energy transfer to the local dissociative S_1 state of azide **1** can also occur through the Dexter (exchange) mechanism.[45] In this case, the excited state of the aryl azide moiety will be formed. According to the recent femtosecond pump−probe experiments,[51] upon excitation phenyl azide and a series of its derivatives undergo dissociation to molecular nitrogen and singlet arylnitrene on a femtosecond time scale (100−500 fs). Thus, in the case of the energy transfer, the singlet arylnitrene will be formed after completion of quenching process.

Results of our ultrafast pump−probe experiments unambiguously demonstrate that quenching of local pyrene fluorescence in the covalently linked systems **2** and **3** cannot be described as a simple exponential decay. The decay of the local pyrene S_1 state is well described by a two exponential function. Furthermore, pyrene radical cations were found to be mainly formed in a process with a shorter time constant (∼26 ± 5 ps for **2** and 46 ± 15 ps for **3**).

We can give the following reasonable explanation of our results. First of all, it should be proposed that both processes, electron transfer to the aryl azide moiety and energy transfer to the local dissociative S_1 state of aryl azide, are important. Moreover, electron transfer dominates in the "short time" process and energy transfer in the "long time" process. Most likely, two observed time constants correspond to quenching in different conformers of covalently linked systems, e.g., conformers **2A** and **2B** in the case of **2** (Figure 2). Though these conformers have essentially the same distances between centers of pyrene and aryl azide moieties (∼7.9 Å), orientations of the moieties differ significantly (Figure 2). For instance, dihedral angles between the planes of two moieties are predicted to be ∼120° (**2A**) and ∼90° (**2B**).

In the case of nonadiabatic electron transfer, the prefactor A in formula (1) is proportional to the square of the electronic coupling matrix element H_{RP}.[39,40] The value of H_{RP} is predicted to fall off exponentially with the distance because of exponential decay of electronic wave functions of the donor and acceptor.[39,40] It has been also recognized that H_{RP} depends upon mutual donor−acceptor orientation as well as the overall conformation of the linked system.[53,54] Furthermore, in some cases dramatically different photophysical properties were observed for conformers with the same donor−acceptor distances.[54] Note that oscillator strengths of the transition to CT_1 state also depend on mutual orientation and differ by about three times for the conformers **2A** and **2B** (Table S2).

As mentioned above, energy transfer is proposed to occur mainly on the longer time scale. However, we were unable to detect formation of the singlet nitrene **5S**. This can be explained taking into account that **5S** has much lower absorption in the visible region than pyrene radical cation. Indeed, according to the calculations, oscillator strength of the most intense absorption band of phenylnitrene in the near-UV region is about 10 times smaller (∼0.03)[14b] than that of ^{2}Pyr$^+$ (0.35, Figure 10).

SCHEME 3

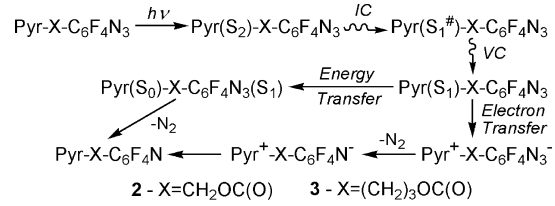

As in the case of electron transfer, the rate constant of the energy transfer by Dexter mechanism is predicted to fall off exponentially with the distance.[45] The distances between moieties in the low energy conformers of **3** are longer than those of **2** by more than 2 Å. The distance dependence of the proposed energy transfer rate constant contributes mainly to the difference of the time constants in the systems **2** and **3** (∼140 ± 20 ps and 810 ± 90 ps, respectively).

Clearly the present interpretation of our results requires further studies to clarify the complexity caused by occurrence of the two quenching mechanisms and coexistence of different conformers. Using solvents of different polarity and linked systems with various aryl azide moieties, we can alter the relative efficiency of the proposed quenching processes. The rate constant of energy transfer is expected to be independent of solvent polarity.[55]

5. Conclusions

A comprehensive and quantitative mechanism of the primary physical and chemical processes which follow photoexcitation of the covalently linked systems, 1-[(4-azido-2,3,5,6-tetrafluorobenzoyloxy)methyl]pyrene (**2**) and 1-[3-(4-azido-2,3,5,6-tetrafluorobenzoyloxy)propyl]pyrene (**3**), has been established using femto- and nanosecond transient absorption spectroscopy and computational chemistry (Scheme 3).

Excitation of **2** and **3** at 336 nm results in the population of the second excited singlet state of the pyrene moiety (S_2). Internal conversion (IC) to the lowest singlet excited state of a pyrene moiety (S_1) occurs with a time constant of ∼140 fs, a value which is similar to that of unsubstituted pyrene. The lowest singlet excited state of the pyrene moiety undergoes vibrational cooling (VC) with a time constant ∼2 ps which agrees with that of pyrene itself.

The decay of the local pyrene S_1 state measured in the pump−probe experiments was approximated by a two exponential process with time constants which agree well with the values obtained previously from the fluorescence decay kinetics.[17] The transient absorption spectra detected after completion of quenching of the local pyrene excited states (S_1) of both systems **2** and **3** have been assigned to the radical cation of the pyrene moiety. Moreover, pyrene radical cations were mainly formed on the shorter time scale (∼26 ± 5 ps for **2** and 46 ± 15 ps for **3**). Most likely, both electron transfer (ET) and energy transfer from pyrene to the aryl azide moiety are responsible for the quenching of the local pyrene fluorescence.

Acknowledgment. Ultrafast studies were performed at the Ohio State University Center for Chemical and Biophysical Dynamics. Support of this work by the National Science Foundation (Supplementary Grant to CHE-0237256), Russian Foundation for Basic Research (Grant 09-03-00410) and by the Ohio Supercomputer Center are gratefully acknowledged.

Supporting Information Available: Part 1: Active space used in the CASSCF/CASPT2 calculations of the electronic

transitions in pyrene (Figure S1) and their energies (Table S1), energies and oscillator strengths of transition to the CT_1 state for different conformers of **2** and **3** (Table S2), UV−vis spectra of pyrene and pyren-1-ylmethanol (Figure S2), the structures of selected conformers of **3** (Figures S3, S4), geometry of aryl azide **1** and its radical anion calculated by the B3LYP/6-31+G(d) method (Figure S5), global fitting results (Figures S6 and S9, Tables S3−S5), normalized transient absorption spectra (Figure S7), analysis of kinetics for **2** on the picosecond time scale (Figure S8), decay associated spectra obtained for **3** (Figure S10), persistent spectrum of the triplet nitrene **5T** detected after brief photolysis of **1** at 77 K (Figure S11), the difference spectrum recorded upon stationary photolysis of **2** at 298 K (Figure S12). Part 2: Cartesian coordinates and energies of all stationary points located in this study. This material is available free of charge via the Internet at http://pubs.acs.org.

References and Notes

(1) (a) Branner, K. *Annu. Rev. Biochem.* **1993**, *62*, 483. (b) Meisenheimer, K. M.; Koch, T. H. *Crit. Rev. Biochem. Mol. Biol.* **1997**, *32*, 101–140. (c) Knorre, D. G.; Godovikova, T. S. *FEBS Lett.* **1998**, *433*, 9.

(2) Hanna, M. M.; Meares, C. F. *Biochemistry* **1983**, *22*, 3546.

(3) (a) Renfron, M. B.; Naryshikin, N.; Lewis, L. M.; Chen, H.-T.; Ebright, R. H.; Scott, R. A. *J. Biol. Chem.* **2004**, *279*, 2825. (b) Dissinger, S.; Hanna, M. M. *J. Biol. Chem.* **1990**, *265*, 7662.

(4) Buchmueller, K. L.; Weeks, K. M. *Biochemistry* **2003**, *42*, 13869.

(5) Hixson, S. H.; Hixson, S. S. *Biochemistry* **1975**, *14*, 4251.

(6) (a) Ofengand, J.; Schwartz, I.; Chinali, G.; Hixson, S. S.; Hixson, S. H. *Methods Enzymol.* **1977**, *46*, 683. (b) Burgin, A. B.; Pace, N. R. *EMBO J.* **1990**, *9*, 4111. (c) Wang, J.-F.; Downs, W. D.; Cech, T. R. *Science* **1993**, *260*, 504.

(7) (a) Costas, C.; Yuriev, E.; Meyer, K. L.; Guion, T. S.; Hanna, M. M. *Nucleic Acids Res.* **2000**, *28*, 1849. (b) Niranjanakumari, S.; Stams, T.; Crary, S. M.; Christianson, D. W.; Fierke, C. A. *Proc. Natl. Acad. Sci.* **1998**, *95*, 15212.

(8) Sylvers, L. A.; Wower, J. *Bioconjugate Chem.* **1993**, *4*, 411.

(9) (a) Lannotti, B. J.; Persinger, J.; Bartholomew, B. *Biochemistry* **1996**, *35*, 9821. (b) Doerhoefer, S.; Khodyreva, S.; Safronov, I. V.; Vlassoff, W. A.; Anarbaev, R.; Lavrik, O. I.; Holler, E. *Microbiology* **1998**, *144*, 3181. (c) Lavrik, O. I.; Prasad, R.; Sobol, R. W.; Horton, J. K.; Ackerman, E. J.; Wilson, S. H. *J. Biol. Chem.* **2001**, *276*, 25541.

(10) Hanna, M. M.; Bentsen, L.; Lucido, M.; Sapre, A. *Methods Enzymol.* **1989**, *180*, 383.

(11) Kinter, M.; Sherman, N. E. *Protein Sequencing and Identification Using Tandem Mass Spectrometry*; Wiley-Interscience: New York, 2000. (b) Hatanaka, Y.; Sadakane, Y. *Curr. Top. Med. Chem.* **2002**, *2*, 271.

(12) (a) Dobrikov, M. I.; Gaidamakov, S. A.; Gainutdinov, T. I.; Koshkin, A. A.; Vlassov, V. V. *Antisense Nucl. Acid Drug Dev.* **1997**, *7*, 309. (b) Dobrikov, M. I. *Russ. Chem. Rev.* **1999**, *68*, 1062.

(13) (a) Kolpashchikov, D. M.; Rechkunova, N. I.; Dobrikov, M. I.; Khodyreva, S. N.; Lebedeva, N. A.; Lavrik, O. I. *FEBS Lett.* **1999**, *448*, 141. (b) Lavrik, O. I.; Kolpachnikov, D. M.; Prasad, R.; Sobol, R. W.; Wilson, S. H. *Nucleic Acids Res.* **2002**, *30*, e73. (c) Maltseva, E. A.; Rechkunova, N. I.; Petruseva, I. O.; Vermeulen, W.; Scharer, O. D.; Lavrik, O. I. *Bioorg. Chem.* **2008**, *36*, 77.

(14) (a) Schuster, G. B.; Platz, M. S. *Adv. Photochem.* **1992**, *17*, 69. (b) Gritsan, N. P.; Zendong, Z.; Hadad, C. M.; Platz, M. S. *J. Am. Chem. Soc.* **1999**, *121*, 1202. (c) Borden, W. T.; Gritsan, N. P.; Hadad, C. M.; Karney, W. L.; Kemnitz, C. R.; Platz, M. S. *Acc. Chem. Res.* **2000**, *33*, 765. (d) Gritsan, N. P.; Platz, M. S. *Adv. Phys. Org. Chem.* **2001**, *36*, 255. (e) Gritsan, N. P.; Platz, M. S.; Borden, W. T. In *Computational Methods in Photochemistry*; Kutateladze, A. G., Ed.; Talor & Francis: Boca Raton, FL, 2005; pp 235−356. (f) Platz, M. S. In *Reactive Intermediate Chemistry, Part 1*; Moss, R. A., Platz, M. S., Jones, M., Eds.; John Wiley & Sons: Hoboken, 2004; pp 501−560. (g) Gritsan, N. P.; Platz, M. S. *Russ. Chem. Rev.* **2007**, *76*, 1139.

(15) (a) McDonald, R. N.; Chowduri, A. K. *J. Am. Chem. Soc.* **1980**, *102*, 5118. (b) Herbranson, D.; Hawley, M. *J. Org. Chem.* **1990**, *55*, 4297. (c) Warrier, M.; Lo, M. K. F.; Monbouquette, H.; Garcia-Garibay, M. A. *Photochem. Photobiol. Sci.* **2004**, *3*, 859.

(16) Kamyshan, S. V.; Litvinchuk, S. V.; Korolev, V. V.; Eremenko, S. I.; Tsentalovich, Yu. P.; Gritsan, N. P. *Kinet. Catal.* **2006**, *47*, 75.

(17) Barabanov, I. I.; Pritchina, E. A.; Takaya, T.; Gritsan, N. P. *Mend. Commun.* **2008**, *18*, 273.

(18) Katritzky, A. R.; Yang, Z.; Lam, J. N.; Nagel, C. *Org. Prep. Proced. Int.* **1998**, *30*, 203.

(19) Stien, D.; Gastaldi, S. *J. Org. Chem.* **2004**, *69*, 4464.

(20) (a) Mykaiyama, T.; Usui, M.; Shimada, E.; Saigo, K. *Chem. Lett.* **1975**, 1045. (b) Han, S.-Y.; Kim, Y.-A. *Tetrahedron* **2004**, *60*, 2447.

(21) Scriven, E. F. V.; Turnbull, K. *Chem. Rev.* **1988**, *88*, 297.

(22) (a) Lippert, E.; Nagele, W.; Seibold-Blankenstein, I.; Staiger, U.; Voss, W. *Z. Analyt. Chem.* **1959**, *170*, 1. (b) Melhuish, W. H. *J. Phys. Chem.* **1960**, *64*, 762.

(23) Burdzinski, G.; Hackett, J. C.; Wang, J.; Gustafson, T. L.; Hadad, C. M.; Platz, M. S. *J. Am. Chem. Soc.* **2006**, *128*, 13402.

(24) Lessing, H. E.; Jena, A. V. *Chem. Phys. Lett.* **1976**, *42*, 213.

(25) Nakayama, T.; Amijima, Y.; Ibuki, K.; Hamanoue, K. *Rev. Sci. Instrum.* **1997**, *68*, 4364.

(26) Tsao, M.-L.; Gritsan, N. P.; James, T. R.; Platz, M. S.; Hrovat, D.; Borden, W. T. *J. Am. Chem. Soc.* **2003**, *125*, 9343.

(27) (a) Becke, A. D. *J. Chem. Phys.* **1993**, *98*, 5648. (b) Lee, C.; Yang, W.; Parr, R. G. *Phys. Rev. B* **1988**, *37*, 785.

(28) Dreuw, A.; Head-Gordon, M. *Chem. Rev.* **2005**, *105*, 4009.

(29) Frisch, M. J. A. *Gaussian 03*, revision B.01; Gaussian, Inc.: Pittsburgh, PA, 2003 (Full reference is given in the Supporting Information).

(30) Tomasi, J.; Mennucci, B.; Cammi, R. *Chem. Rev.* **2005**, *105*, 2999.

(31) Andersson, K.; Roos, B. O. *CASPT2*, 1995, Singapore.

(32) Pierloot, K.; Dumez, B.; Widmark, P.-O.; Roos, B. O. *Theor. Chim. Acta.* **1995**, *90*, 87.

(33) Andersson, K.; Blomberg, M. R. A.; Fülscher, M. P.; Kellö, V.; Lindh, R.; Malmqvist, P.-Å.; Noga, J.; Olson, J.; Roos, B. O.; Sadlej, A.; Siegbahn, P. E. M.; Urban, M.; Widmark, P.-O. MOLCAS, 1994.

(34) Roos, B. O.; Andersson, K.; Fülscher, M. P.; Serrano-Andrés, L.; Pierloot, K.; Merchan, M.; Molina, V. *J. Mol. Struct. (Theochem)* **1996**, *388*, 257.

(35) Birks, J. B. *Photophysics of Aromatic Molecules*; Wiley-Interscience: New York, 1970; pp 121−131.

(36) Foggi, P.; Pettini, L.; Santa, I.; Righini, R.; Califano, S. *J. Phys. Chem.* **1995**, *99*, 7439.

(37) Neuwahl, F. V. R.; Foggi, P. *Laser Chem.* **1999**, *19*, 375.

(38) Raytchev, M.; Pandurski, E.; Buchvarov, I.; Modrakowski, C.; Fiebig, T. *J. Phys. Chem. A* **2003**, *107*, 4592.

(39) (a) Marcus, R. A. *J. Chem. Phys.* **1956**, *24*, 966. (b) Marcus, R. A. *Annu. Rev. Phys. Chem.* **1964**, *15*, 155. (c) Rem, D.; Weller, A. *Isr. J. Chem.* **1970**, *8*, 259. (d) Closs, G. L.; Miller, J. R. *Science* **1988**, *240*, 440. (e) *Photoinduced Electron Transfer*; Fox, M. A., Chanon, M., Eds.; Elsevier: Amsterdam, 1988; Parts A-D. (f) *Electron Transfer in Inorganic, Organic, and Biological Systems*; Bolton, J. R., Mataga, N., McLendon, G., Eds.; Advances in chemistry Series 228; ASC: Washington, DC, 1991. (g) Barbara, P. F.; Meyer, T. J.; Ratner, M. A. *J. Phys. Chem.* **1996**, *100*, 13148.

(40) (a) Marcus, R. A. *Rev. Mod. Phys.* **1993**, *65*, 599. (b) Newton, M. D.; Sutin, N. *Annu. Rev. Phys. Chem.* **1984**, *35*, 437. (c) Newton, M. D. *Chem. Rev.* **1991**, *91*, 767. (d) Schatz, G. C. ; Ratner, M. A. *Quantum Mechanics in Chemistry*; Prentice-Hall: Englewood Cliffs, NJ, 1993.

(41) (a) Baizer, M. B. *Organic Electrochemistry*; Marcel Dekker: New York, 1973. (b) *Encyclopedia of Electrochemistry of the Elements*; Everson, P. E., Ed.; Marcel Dekker: New York, 1979; Vol. XIII.

(42) Shields, C. J.; Falvey, D. E.; Schuster, G. B.; Buchardt, O.; Nielsen, P. E. *J. Org. Chem.* **1988**, *53*, 3501.

(43) Hostein, T. *Philos. Mag. B.* **1978**, *37*, 499.

(44) (a) Burdzinski, G.; Hackett, J. C.; Wang, J.; Gustafson, T. L.; Hadad, C. M.; Platz, M. S. *J. Am. Chem. Soc.* **2006**, *128*, 13402. (b) Budyka, M. F.; Zyubina, T. S. *Zh. Fiz. Khim.* **1998**, *72*, 1420. (c) Budyka, M. F. *High Ehergy Khim.* **2007**, *41*, 176.

(45) Dexter, D. L. *J. Chem. Phys.* **1953**, *21*, 836.

(46) (a) Laermar, F.; Elsaesser, T.; Kaiser, W. *Chem. Phys. Lett.* **1989**, *156*, 38. (b) Miyasaka, H.; Hagihiro, M.; Okada, T.; Mataga, N. *Chem. Phys. Lett.* **1992**, *188*, 259. (c) Schwarzer, D.; Troe, J.; Votsmeier, M.; Zerezke, M. *J. Chem. Phys.* **1996**, *105*, 3121.

(47) (a) Wong, V.; Gruebele, M. *J. Phys. Chem. A* **1999**, *103*, 10664. (b) Kovalenko, S. A.; Schanz, R.; Hennig, H.; Ernsting, N. P. *J. Chem. Phys.* **2001**, *115*, 3256. (c) Gruebele, M. *Adv. Chem. Phys.* **2001**, *114*, 193. (d) Kovalenko, A.; Eilers-Ko1nig, N.; Senyushkina, T. A.; Ernsting, N. P. *J. Phys. Chem. A* **2001**, *105*, 4834. (e) Burdzinski, G.; Maciejewski, A.; Buntinx, G.; Poizat, O.; Lefumeux, C. *Chem. Phys. Lett.* **2003**, *368*, 745. (f) Pritchina, E. A.; Gritsan, N. P.; Burdzinski, G. T.; Platz, M. S. *J. Phys. Chem. A* **2007**, *111*, 10483.

(48) Gritsan, N. P.; Gudmundsdóttir, A. D.; Tigelaar, D.; Zhu, Z.; Karney, W. L.; Hadad, C. M.; Platz, M. S. *J. Am. Chem. Soc.* **2001**, *123*, 1951.

(49) (a) Marcinek, A.; Platz, M. S.; Chan, S. Y.; Floresca, R.; Rajagopalan, K.; Golinski, M.; Watt, D. *J. Phys. Chem.* **1994**, *98*, 412. (b) Gritsan, N. P.; Zhai, H. B.; Yuzawa, T.; Karweik, D.; Brooke, J.; Platz, M. S. *J. Phys. Chem. A.* **1997**, *101*, 2833. (c) Polshakov, D. A.; Tsentalovich, Yu. P.; Gritsan, N. P. *Russ. Chem. Bull.* **2000**, *49*, 50. (d) Polshakov, D. A.; Tsentalovich, Yu. P.; Gritsan, N. P. *Kinetics and Catalysis* **2001**, *42*, 601.

(50) (a) Birnbaum, P. P.; Linford, J. H.; Style, D. W. G. *Trans. Faraday Soc.,* **1953**, *49*, 735. (b) Briquet, L.; Vercauteren, D. P.; Andre, J.-M.; Perpete, E. A.; Jacquemin, D. *Chem. Phys. Lett.* **2007**, *435*, 257.

(51) (a) Gritsan, N. P.; Polshakov, D.; Tsao, M.-L.; Platz, M. S. *Photochem. Photobiol. Sci.* **2005**, *4*, 23. (b) Burdzinski, G.; Gustafson, T. L.; Hackett, J. C.; Hadad, C. M.; Platz, M. S. *J. Am. Chem. Soc.* **2005**, *127*, 13764. (c) Burdzinski, G.; Hackett, J. C.; Wang, J.; Gustafson, T. L.; Hadad, M. C.; Platz, M. S. *J. Am. Chem. Soc.* **2006**, *128*, 13402. (d) McCulla, R. D.; Burdzinski, G.; Platz, M. S. *Org. Lett.* **2006**, *8*, 1637. (e) Burdzinski, G.; Middleton, C. T.; Gustafson, T. L.; Platz, M. S. *J. Am. Chem. Soc.* **2006**, *128*, 14804.

(52) Zanini, G. P.; Montejano, H. A.; Cosa, J. J.; Previtali, C. M. *J. Photochem. Photobiol. A: Chem.* **1997**, *109*, 9.

(53) (a) Cave, R. J.; Siders, P.; Marcus, R. A. *J. Phys. Chem.* **1986**, *90*, 1436. (b) Khundkar, L. R.; Perry, J. W.; Hanson, J. E.; Dervan, P. B. *J. Am. Chem. Soc.* **1994**, *116*, 9700. (c) Toutounji, M. M.; Ratner, M. M. *J. Phys. Chem. A* **2000**, *104*, 8566. (d) Rubtsov, I. V.; Redmore, N. P.; Hochstrasser, R. M.; Therien, M. J. *J. Am. Chem. Soc.* **2004**, *126*, 2684.

(54) (a) Helms, A.; Heiler, D.; McLendon, G. *J. Am. Chem. Soc.* **1991**, *113*, 4325. (b) Daub, J.; Engl, R.; Kurzawa, J.; Miller, S. E.; Schneider, S.; Stockmann, A.; Wasielewski, M. R. *J. Phys. Chem. A* **2001**, *105*, 5655. (f) Acar, N.; Kurzawa, J.; Fritz, N.; Stockmann, A.; Roman, C.; Schneider, S.; Clark, T. *J. Phys. Chem. A* **2003**, *107*, 9530.

(55) Yeow, E. K. L.; Ziolek, M.; Karolczak, J.; Shevyakov, S. V.; Asato, A. E.; Maciejewski, A.; Steer, R. P. *J. Phys. Chem. A* **2004**, *108*, 10980.

JP901157S